PERGAMON

International Journal of Heat and Mass Transfer 41 (1998) 3627–3634

International Journal of HEAT and MASS TRANSFER

Direct numerical simulation of a turbulent channel flow with a linear spanwise mean temperature gradient

Koji Matsubara*, Mutsuo Kobayashi, Hiroshi Maekawa

Faculty of Engineering, Niigata University, Ikarashi 2-nocho 8050, Niigata 950-21, Japan

Received 14 October 1997

Abstract

Spanwise heat transfer in wall turbulence was studied in a turbulent channel flow having a linear spanwise variation of time-mean temperature just the same as the spanwise variation of wall-temperature. The results of direct numerical simulation (DNS) for various Prandtl numbers ranging from 0.1–1.5 were compared with existing DNS data for ordinary two-dimensional heat transfer from uniformly heated walls. The Prandtl number effect on the spanwise eddy diffusivity of heat was found to be quite similar to that on the wall-normal component. Similarity was also observed between the destruction of the spanwise turbulent heat flux and that of the wall-normal component.

Nomenclature

C_p specific heat at constant pressure [J kg^{-1} K^{-1}]
i unit vector in x direction
k turbulent kinetic energy [m^2 s^{-2}]
L_x, L_z computational domain size in x and z directions [m]
p pressure fluctuation [Pa]
P pressure deviating from P_x [Pa]
P_x pressure component generating driving force $=(\rho U_\tau^2/\delta)x+$const. [Pa]
Pr Prandtl number $=\rho C_p \nu/\lambda$
$Q_{\phi\psi}$ correlation coefficient $=|\overline{\phi\psi}|/(\phi_{rms}\psi_{rms})$
Re Reynolds number $=U_\tau\delta/\nu$
t time [s]
T temperature [K]
u, v, w velocity fluctuation in x, y and z directions [m s^{-1}]
U, V, W velocities in x, y and z directions [m s^{-1}]
U_τ friction velocity [m s^{-1}]
V velocity vector $=(U, V, W)$ [m s^{-1}]
x, y, z coordinates in streamwise, wall-normal and spanwise directions [m]
x_i coordinate in ith direction; x_1, x_2 and x_3 denote x, y and z, respectively [m].

Greek symbols
δ channel half width [m]
Δt time step [s]
Δx, Δy, Δz grid spacings in x, y and z directions [m]
ε dissipation rate of k [m^2 s^{-3}]
ε_{hy} wall-normal eddy diffusivity of heat [$\overline{\text{m}^2}$ s^{-1}]
ε_{hz} spanwise eddy diffusivity of heat $=-\overline{w\theta}/(\mathrm{d}\langle T\rangle/\mathrm{d}z)$ [m^2 s^{-1}]
ε_m kinematic eddy viscosity $=-\overline{uv}/(\mathrm{d}\bar{U}/\mathrm{d}y)$ [m^2 s^{-1}]
ε_θ dissipation rate of $\overline{\theta^2}$ [K^2 s^{-1}]
θ temperature fluctuation [K]
Θ temperature deviating from T_W [K]
λ thermal conductivity [W m^{-1} K^{-1}]
ν kinematic viscosity [m^2 s^{-1}]
ρ density [kg m^{-3}]
τ dissipation time scale of velocity fluctuation $=k/\varepsilon$ [s]
τ_θ dissipation time scale of temperature fluctuation $=\overline{\theta^2}/\varepsilon_\theta$ [s].

Superscripts and subscripts
$()^+$ non-dimensionalization with U_τ, ν and ρ
$()^*$ non-dimensionalization with U_τ, δ and $\mathrm{d}T_W/\mathrm{d}z$
$(\bar{})$ ensemble average
$()_W$ wall.

Miscellaneous
∇ nabla $=(\partial/\partial x^*, \partial/\partial y^*, \partial/\partial z^*)$
$\langle\,\rangle$ time mean.

* Corresponding author.

0017–9310/98 $19.00
PII: S0017–9310(98)00072–6

1. Introduction

Spanwise or circumferential transfer of heat and mass in wall turbulent flows plays an important role in many practical applications. Therefore, several experimental studies were performed for this type of heat transfer [1–5], and some closure expressions were proposed for the spanwise turbulent heat flux or the spanwise eddy diffusivity of heat [3, 6, 7]. Early contributions to this topic were made by Black and Sparrow [1] and Quarmby and Quirk [2]. They studied experimentally non-axisymmetric transfer of passive scalar quantities in a circular pipe, and reported that the circumferential eddy diffusivities of heat and mass are much larger than the wall-normal components in the vicinity of the wall. Maekawa and his colleagues [3–5] performed a series of experimental studies in a turbulent boundary layer of air flow where the main-stream temperature varied linearly in the spanwise direction. According to Maekawa et al. [3], the ratio of the spanwise eddy diffusivity of heat to the kinematic eddy viscosity, $\varepsilon_{hz}/\varepsilon_m$, is almost constant away from the wall, but it increases rapidly in the vicinity of the wall. These experimental studies contributed towards clarification of the fundamental aspects of spanwise heat transfer. However, quantitative accuracy of the existing experimental data should not be high enough to examine the prediction performance of the related closure expressions. For example, the distribution of spanwise eddy diffusivity of heat reported by Quarmby and Quirk [2] contains extremely wide scatter, and insufficient accuracy of the experimental data was thus suggested.

In the previous study [8], direct numerical simulation (DNS) was performed for a turbulent channel flow having linear spanwise non-uniformity of time-mean temperature equal to the spanwise variation of wall temperature. This flow system is somewhat artificial but offers a good arena for the discussion of the detailed features of spanwise heat transfer. The numerical data demonstrated that there is rough agreement between the distributions of $\varepsilon_{hz}/\varepsilon_m$ and the ratio of spanwise and wall-normal components of Reynolds normal stresses, supporting the algebraic expressions giving the spanwise eddy diffusivity of heat proposed by Launder [6] and Maekawa et al. [3]. As an extension of the previous study, Prandtl number effects are further examined in order to obtain deeper insights into the spanwise heat transfer and to provide more detailed data that can be used to investigate the reliability of the related turbulence models. The computational results are discussed in comparison with the existing DNS data for an ordinary two-dimensional heat transfer in a channel with uniform wall heating.

2. Computational method

The presently used computational domain and coordinate system are shown in Fig. 1. The streamwise, wall-normal and spanwise coordinates are denoted by x, y and z, respectively. The wall temperature, T_W, is assumed to be uniform in the streamwise direction but to vary linearly in the spanwise direction. The flow and thermal fields are assumed to be fully developed. In this situation, the time-mean temperature, $\langle T\rangle$, is uniform in the x and y directions but has a linear spanwise non-uniformity equal to $\mathrm{d}T_W/\mathrm{d}z$. Therefore, turbulence statistics depend solely on the distance from the wall. The working fluid is assumed to be a Newtonian fluid with constant properties. Temperature is treated as a passive scalar. Under these assumptions, the continuity, Navier–Stokes and energy equations are described, respectively, as

$$\nabla\cdot\mathbf{V}^+ = 0 \tag{1}$$

$$\frac{\partial\mathbf{V}^+}{\partial t^*} + (\mathbf{V}^+\cdot\nabla)\mathbf{V}^+ = -\nabla P^+ + \frac{1}{Re}\nabla^2\mathbf{V}^+ + \mathbf{i} \tag{2}$$

$$\frac{\partial\Theta^*}{\partial t^*} + (\mathbf{V}^+\cdot\nabla)\Theta^* = \frac{1}{Re\,Pr}\nabla^2\Theta^* - W^+ \tag{3}$$

where all variables are non-dimensionalized with friction velocity, U_τ, channel half width, δ, density, ρ, and $\mathrm{d}T_W/\mathrm{d}z$. A constant pressure gradient is provided to drive the channel flow, and its non-dimensional form corresponds to the last term on the right hand side of equation (2), $\mathbf{i}$. The temperature, T, is decomposed into the wall temperature, T_W, and its deviation from T_W, Θ. The last term on the right hand side of equation (3), $-W^+$, appears due to this decomposition. It is equivalent to $-W^+\mathrm{d}T^*/\mathrm{d}z^*$, and $\mathrm{d}T^*/\mathrm{d}z^*$ is equal to unity. Here W^+ is the non-dimensional velocity component in the spanwise direction.

Spatial periodicity was assumed in describing the boundary conditions for the streamwise and spanwise directions. On the wall, pressure was computed using the compatibility condition

$$\frac{\partial P^+}{\partial y^*} = \frac{1}{Re}\frac{\partial^2 V^+}{\partial y^{*2}} \tag{4}$$

derived from equation (2), where V^+ is the non-dimensional velocity component in the wall-normal direction. The temperature fluctuation on the wall was fixed at zero as was done in the existing DNS performed by Kasagi and Ohtsubo [9] and Kim and Moin [10].

The finite difference approach is used in the present DNS. Fourth-order finite differencing is used for all the spatial derivatives in equations (2) and (3). The finite differencing of the convection term in the Navier–Stokes equation is made following the consistent scheme developed by Kajishima [11] and Suzuki and Kawamura [12] with modification to secure fourth-order accuracy. In the time integration of the resulting equations, the pressure terms are implicitly treated, and the other terms are evaluated by means of the Adams–Bashforth method. The Poisson equation derived from equations (1) and (2) is solved for the pressure. In the derivation of the Poisson

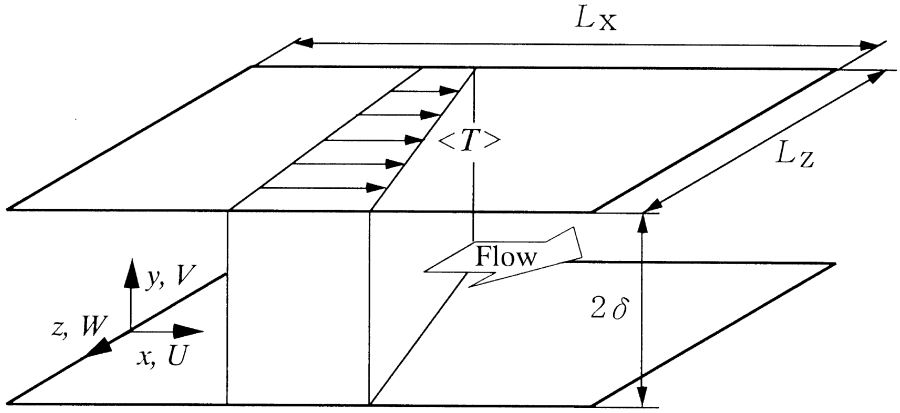

Fig. 1. Computational domain.

equation, the continuity condition (1) was applied for the latest velocity components as was done in the fractional step method and in the MAC (Marker and Cell) method.

The initial value of the streamwise velocity is set to have the mean part following the wall law with random fluctuations superimposed on it. Initial values of the other velocity components, pressure and temperature are all set to be zero. The computation was proceeded observing the first and second moments of dependent variables. After the effect of the initial values fully vanished, ensemble averaging was performed with respect to time and locations. For this purpose, numerical results obtained at positions of equal distance from the wall were included among the data for averaging. The turbulence statistics obtained by this averaging are denoted with an overbar ($^-$) in the following discussion.

The adopted computational conditions are listed in Table 1. The Prandtl number, Pr, is changed in four steps from 0.1–1.5 keeping the Reynolds number, Re ($=U_\tau\delta/\nu$), constant at 150. Total number of $64\times61\times64$ grid points are allocated in the computational domain finely in the neighborhood of the wall. A smaller value of the time step is required for the case of $Pr=0.1$ to suppress the numerical instability more likely to occur for lower values of Pr. In the previous study [8], comparison was made between the mean velocity, various second-order turbulence statistics of the flow field and the turbulence energy budget obtained with the same grid resolution as listed in Table 1 and the counterparts of the DNS data base [13] constructed by reliable simulation with finer grid resolution and the larger computational domain size. There is some discrepancy between both results with respect to the peak value of Reynolds normal stresses, and the decay of two-point correlations was not complete at the separation corresponding to the computational domain half size in comparison with the DNS data base. These suggest that the density of grid allocation and the computational domain size are not large enough in the present computation. However, the general trend of the turbulence statistics agree well with that of the DNS data base, and the discrepancy found in the peak of the Reynolds normal stresses was within five percent. Therefore, computational inaccuracy observed in the flow field confirmed to be not so serious at least in the discussion of low-order turbulence statistics.

Table 1
Computational conditions

Re	150
Pr	0.1, 0.3, 0.71, 1.5
L_x/δ	7.85
L_z/δ	3.14
Grid number	$64\times61\times64$
Δx^+	18.4
Δy^+	1.03–9.51
Δz^+	7.36
Δt^+	0.03 for $Pr=0.1$, 0.06 for others
Averaging time span	$3450\nu/U_\tau^2$

3. Results and discussion

In the flow under discussion, turbulent heat flux only has a spanwise component, $\overline{w\theta}$. Figure 2 shows distributions of $\overline{w\theta}$ for various Prandtl numbers. In this figure, y^+ is the non-dimensional distance from the wall, yU_τ/ν, and $y^+=150$ corresponds to the channel center. Distributions of $\overline{w\theta}$ have mild peaks around $y^+=70$. There exists only a small difference between the distributions of $\overline{w\theta}$ for two cases of $Pr=1.5$ and $Pr=0.71$. However, when Pr is smaller than 0.71, $\overline{w\theta}$ shows remarkable reduction with a decrease of Pr. As described later, these features of $\overline{w\theta}$ reflect the variations in the budget of $\overline{w\theta}$. Since the spanwise gradient of time-mean tem-

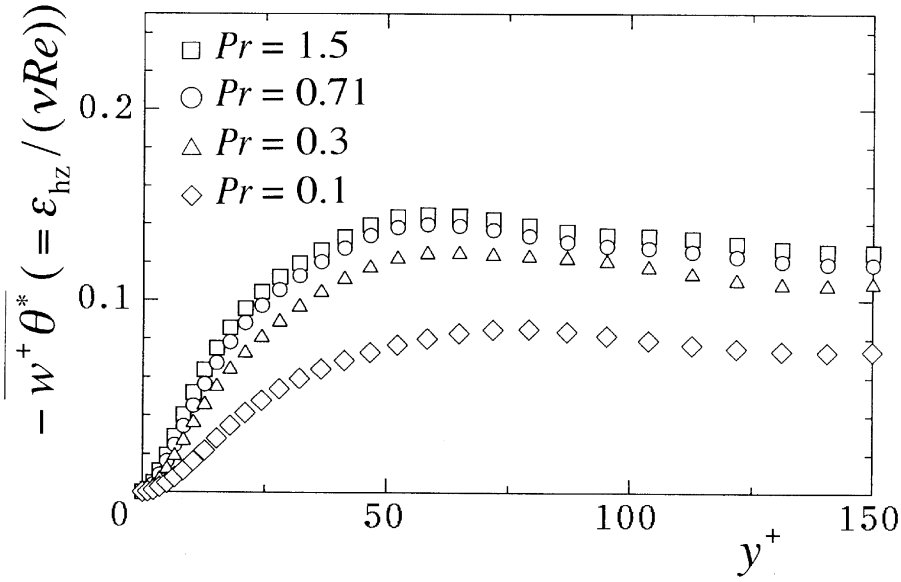

Fig. 2. Distributions of spanwise turbulent heat flux.

perature, $\mathrm{d}\langle T\rangle/\mathrm{d}z$, is uniform throughout the flow field, distributions of $w\theta$ and the corresponding eddy diffusivity of heat, ε_{hz}, are completely similar in shape, and show the same dependency on the value of Pr.

In liquid metal turbulence, it is well known that the wall-normal eddy diffusivity of heat, ε_{hy}, is much smaller than that for fluids with Pr close to unity [9, 14–18]. According to Azer and Chao [14], the temperature fluctuation induced in low Prandtl number turbulence rapidly decays due to strong thermal diffusivity of the fluid. On the other hand, it is also known that change of ε_{hy} as well as that of ε_{hz} is not serious for Pr larger than a critical value [10, 19]. Therefore, the dependency of ε_{hy} or ε_{hz} on the value of Pr shows different features in low and middle ranges of Pr. As shown in references [9, 19] and in the later section of the present paper, this should result from the fact that in the case of the middle range of Pr turbulence mixing plays a more important role in the diminishing of turbulent heat flux than the effect of the thermal diffusivity.

In Fig. 3, comparison is made between two kinds of correlation coefficients, $Q_{w\theta}$ and $Q_{v\theta}$. The latter is the DNS data calculated by Kim and Moin for the case with uniformly heated walls at $Re = 180$ [10]. While the values of $Q_{v\theta}$ take zero at the channel center, the values of $Q_{w\theta}$ are almost constant over the whole width of the channel. However, in the region of $y^+ < 100$, $Q_{w\theta}$ and $Q_{v\theta}$ are roughly equal to each other for the same value of Pr, and together increase slightly with the decrease of Pr.

As observed in Fig. 4, the temperature variance, $\overline{\theta^2}$ reduces as Pr is decreased. The reduction of $\overline{\theta^2}$ arises partly from the decrease in the production rate, $-\overline{w\theta}\,\mathrm{d}\langle T\rangle/\mathrm{d}z$. However, this effect is trivial for Pr larger than 0.71, since $w\theta$ is not substantially affected by the value of Pr at such high values of it. Another point is related with the Prandtl number effect on the dissipation time scale of temperature fluctuation, τ_θ. Figure 5 shows the time scale ratio, τ_θ/τ, where τ is the dissipation time scale of velocity fluctuation. The behavior of τ_θ/τ indicates that the lifetime of temperature fluctuation becomes shorter with the decreasing of Pr. The result of Kasagi and Ohtsubo [9] for the case of uniformly heated walls at $Re = 150$ is also plotted in Fig. 5. Since the temperature fluctuation is assumed to be zero at the wall in both computations, the values of τ_θ/τ are theoretically deduced to

$$\tau_\theta/\tau \to Pr \quad \text{as } y^+ \to 0. \tag{5}$$

Launder [6] examined the behavior of the eddy diffusivity ratio, $\varepsilon_{hz}/\varepsilon_{hy}$, assuming that the spanwise and wall-normal components of turbulent heat flux, $w\theta$ and $v\theta$, are in the local equilibrium and that related fluctuations, w, θ, are of the local isotropy. Due to these assumptions, the pressure–temperature gradient correlation becomes a solitary term balancing with the production term. He approximated this term so as to be proportional to the corresponding turbulent heat flux and derived

$$\varepsilon_{hz}/\varepsilon_{hy} = \overline{w^2}/\overline{v^2}. \tag{6}$$

Here, $\overline{w^2}$ and $\overline{v^2}$ are the spanwise and wall-normal components of the Reynolds normal stress, respectively. Figure 6 shows the eddy diffusivity ratio, $\varepsilon_{hz}/\varepsilon_{hy}$, for the two cases of $Pr = 0.1$ and $Pr = 0.71$, where the data of ε_{hy} is quoted from the DNS result by Kim and Moin [10]. The

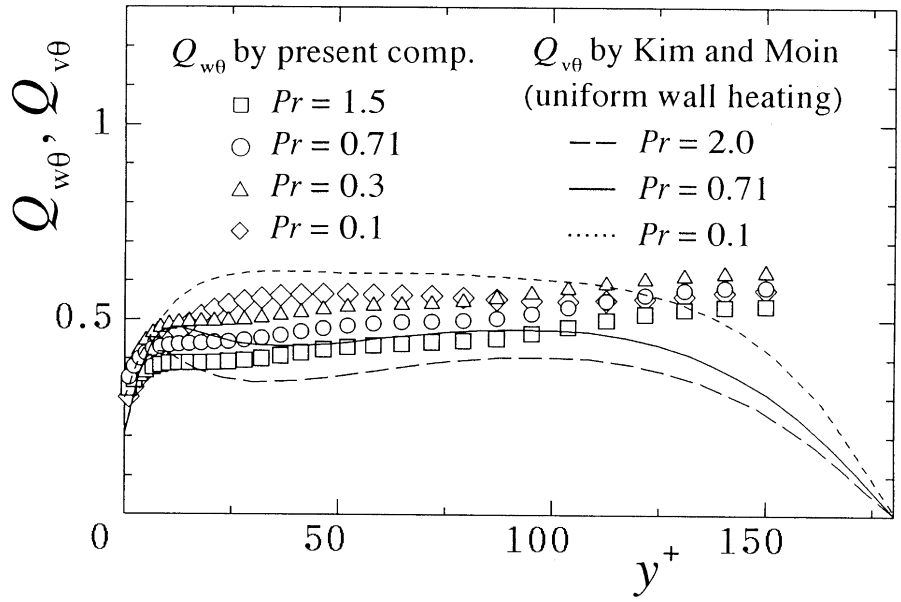

Fig. 3. Distributions of correlation coefficients, $Q_{w\theta}$ and $Q_{v\theta}$.

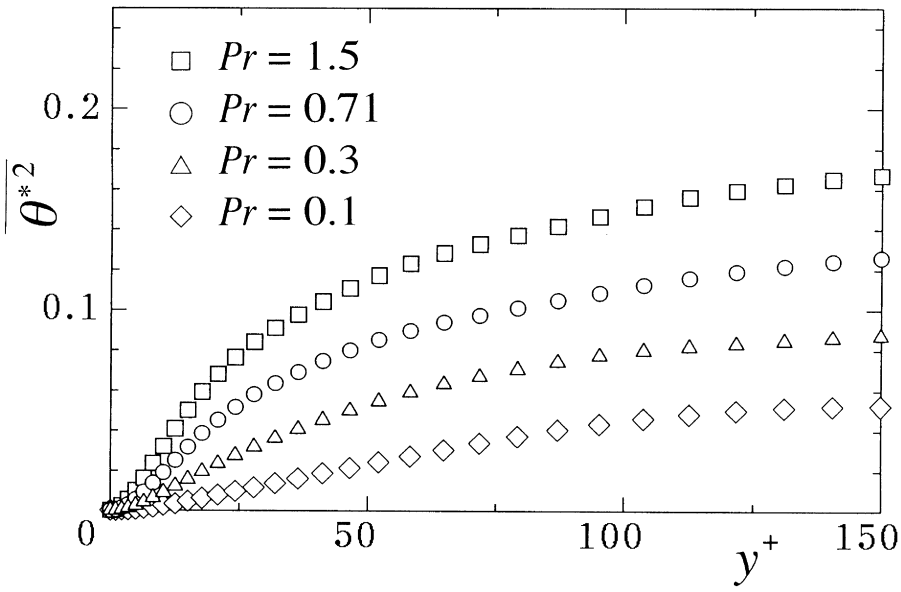

Fig. 4. Distributions of temperature variance.

Reynolds number used by Kim and Moin is 180 and is slightly larger than the present condition. The Reynolds normal stress ratio, $\overline{w^2}/\overline{v^2}$, is also shown in this figure. The distribution of $\overline{w^2}/\overline{v^2}$, indicates the asymptotic behavior of the Reynolds stresses such that $\overline{w^2}$ decreases more gradually than $\overline{v^2}$ when approaching the wall. The value of $\varepsilon_{hz}/\varepsilon_{hy}$ becomes smaller especially in the near-wall region when Pr is decreased. However, there is a rough similarity between distributions of $\varepsilon_{hz}/\varepsilon_{hy}$ and the distribution of $\overline{w^2}/\overline{v^2}$. Thus, equation (6) approximately holds for these values of Pr.

Rogers et al. [7] performed the DNS of homogeneous turbulent shear flow with mean temperature gradients in each of the three orthogonal directions. In their result,

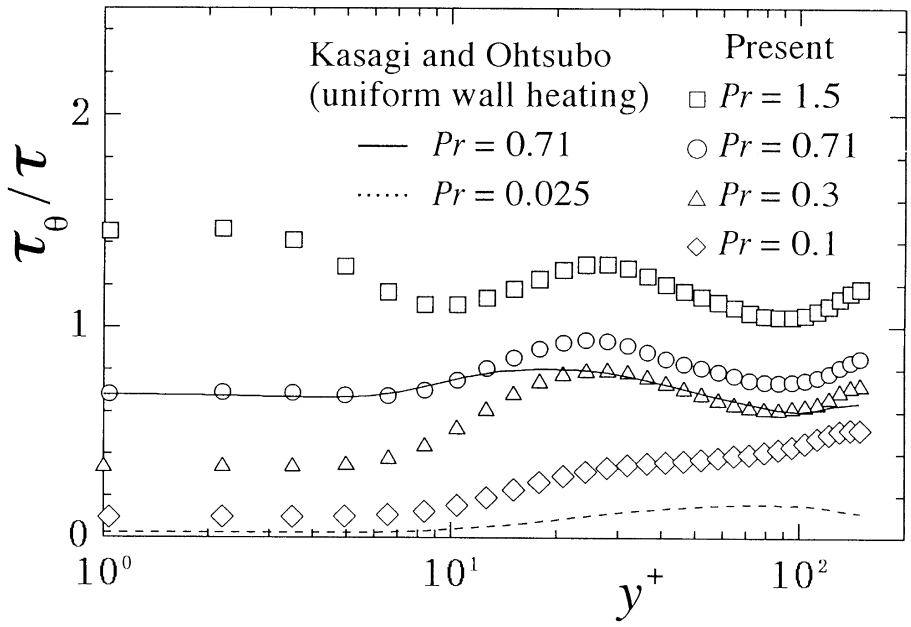

Fig. 5. Distributions of time scale ratio.

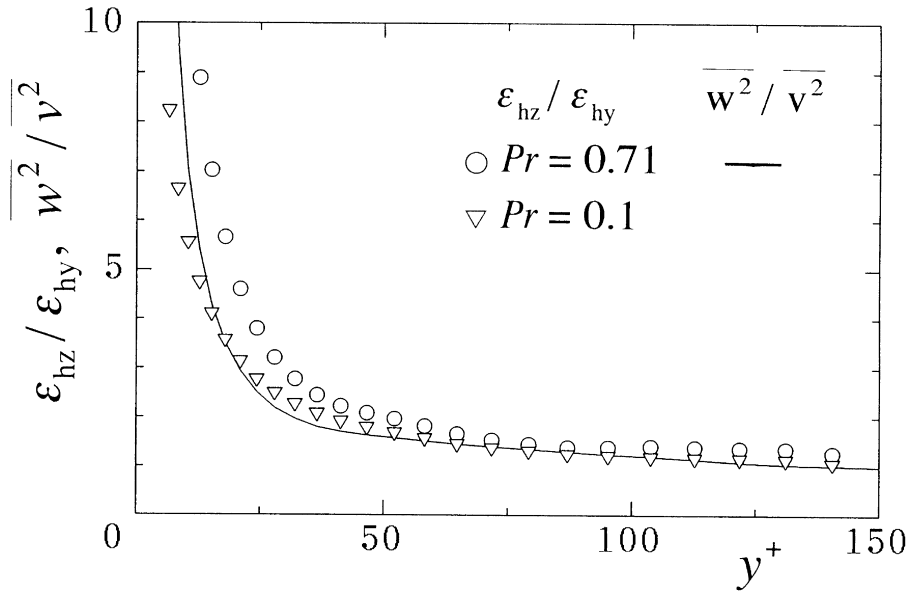

Fig. 6. Distributions of eddy diffusivity ratio and Reynolds normal stress ratio.

the ratio of the spanwise and lateral components of eddy diffusivity of heat changes in time but asymptotically approaches the constant value of approximately 1.6. This result is as large as the present result of $\varepsilon_{hz}/\varepsilon_{hy}$ in the channel central part of $y^+ > 100$.

In the case of the present study, the transport equation of $\overline{w\theta}$ can be written as

$$0 = \underbrace{-\overline{w^{+2}}\frac{\mathrm{d}\langle T^*\rangle}{\mathrm{d}z^+}}_{\text{Production}} \underbrace{-\left(1+\frac{1}{Pr}\right)\overline{\frac{\partial w^+}{\partial x_j^+}\frac{\partial \theta^*}{\partial x_j^+}}}_{\text{Dissipation}} \underbrace{-\frac{\partial}{\partial y^+}(\overline{v^+ w^+ \theta^*})}_{\text{Turbulent diffusion}} \underbrace{+p^+\overline{\frac{\partial \theta^*}{\partial z^+}}}_{\text{Pressure temperature-gradient correlation}}$$

$$+\frac{\partial}{\partial y^+}\underbrace{\left(\overline{\theta^*\frac{\partial w^+}{\partial y^+}}+\frac{1}{Pr}\overline{w^+\frac{\partial \theta^*}{\partial y^+}}\right)}_{\text{Molecular diffusion}}.$$

Figure 7 shows the computational results of each term in equation (7) with the residual of this equation. Since temperature is considered to be a passive scalar in this study, w^2 included in the production rate of $w\theta$ should not depend on Pr. This results in the same distribution of the production rate for different values of Pr. The following three features are common for all the studied cases. (1) In the whole channel width except the viscous sublayer ($y^+ > 5$), the production rate, the pressure–temperature gradient correlation (P–TG) and the dissipation rate are dominant, and $\overline{w\theta}$ is nearly in the local equilibrium. (2) The turbulent diffusion takes a mild peak around $y^+ = 10$, but its peak value is very small compared with the production rate over the whole channel width. (3) In the viscous sublayer of $y^+ < 5$, the molecular diffusion and the dissipation rate balance with each other.

As shown in Fig. 7, P–TG and the dissipation have a sign opposite to the production term, and are supposed to be major processes suppressing excessive growth of the turbulent heat flux. The term destruction is used to denote these processes. In all the cases, the dissipation rate is a dominant term of the total destruction in the region of $y^+ < 10$. In the remaining region, P–TG and the dissipation are competitive processes for the destruction of $\overline{w\theta}$, and their contributions to the total destruction vary dramatically with the change of Pr. In this region, P–TG is distinctively larger than the dissipation for $Pr = 1.5$ and $Pr = 0.71$. Since P–TG corresponds to the destruction through the turbulent mixing, it should be almost independent of Pr. This is consistent with the aforementioned feature of $w\theta$ that its dependency on Pr is weak for Pr larger than 0.71. The contribution of the dissipation to the total destruction grows with decreasing Pr, and becomes dominant over the whole channel width for the case of $Pr = 0.1$. A similar trend of the dissipation was also reported by Iida and Kasagi [20] for the lateral turbulent heat flux in the homogeneous turbulence. According to their discussion, the wave number range where the turbulent heat flux is dissipated shifts to the lower side with the decrease of Pr, but the wave number range in which destruction by turbulence mixing occurs does not basically depend on the value of Pr. This should lead to the increasing rate of the dissipated turbulent heat flux and shortening of the time span from the birth of turbulent heat flux to its dissipation. This effect would cause the reduction of $w\theta$ observed in the present computation.

With regard to the effect of Pr on the destruction of turbulent heat flux, a similar tendency was also found in a turbulent channel flow with uniformly heated walls [19]. The value of Pr for which P–TG or, in contrast, the dissipation dominates the destruction of $\overline{v\theta}$ is roughly equal to the counterpart of the present study. Therefore, in the case of $Pr = 0.71$ where equation (6) was shown

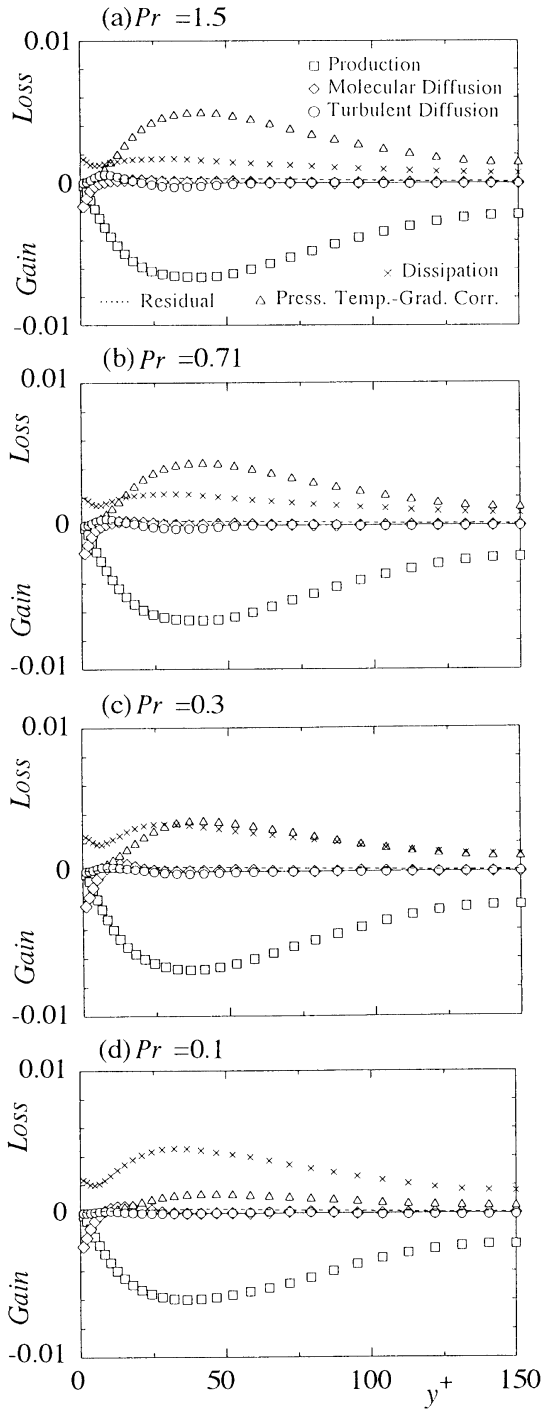

Fig. 7. Budgets of spanwise turbulent heat flux.

to approximately hold, P–TG is larger in the destructions of $\overline{w\theta}$ and $\overline{v\theta}$, and the related fluctuations almost satisfy the local isotropy assumed by Launder in the derivation of equation (6). However, in the case of $Pr = 0.1$ where equation (6) still holds, the dissipation is dominant in the destructions of both $\overline{w\theta}$ and $\overline{v\theta}$. At this value of Pr, the total destruction including the dissipation should match the Launder's approximation made for P–TG, namely that P–TG is proportional to the corresponding turbulent heat flux.

4. Conclusions

Direct numerical simulation (DNS) was performed for the simple case of spanwise heat transfer in wall turbulence, namely a turbulent channel flow with a linear spanwise non-uniformity of time-mean fluid temperature equal to the non-uniformity of the wall temperature. The present results for Prandtl number, Pr, ranging from 0.1–1.5 were compared with the existing DNS data for ordinary two-dimensional heat transfer in a channel flow with uniform wall heating. The following conclusions are derived.

(1) The spanwise eddy diffusivity of heat, ε_{hz}, shows remarkable reduction with decreasing of Pr. This reduction of ε_{hz} is quite similar to the behavior of the wall-normal eddy diffusivity of heat, ε_{hy} in a channel flow with uniformly heated walls.

(2) The eddy diffusivity ratio $\varepsilon_{hz}/\varepsilon_{hy}$ is almost uniform away from the wall, but it changes steeply in the near-wall region. The distribution of $\varepsilon_{hz}/\varepsilon_{hy}$ for both $Pr = 0.71$ and $Pr = 0.1$ roughly agrees with the distribution of the Reynolds normal stress ratio, $\overline{w^2}/\overline{v^2}$. Therefore, the proposition of Launder $\varepsilon_{hz}/\varepsilon_{hy} = \overline{w^2}/\overline{v^2}$ nearly holds in a wide range of Pr.

(3) Since the Reynolds number treated in the present computation is comparatively low, not only the pressure–temperature gradient correlation but also the dissipation take part in the destruction of $\overline{w\theta}$. The contribution of the dissipation to the total destruction increases as Pr decreases. This trend of the dissipation is similar to the counterpart of $\overline{v\theta}$ previously reported in the case of uniform wall heating.

References

[1] Black AW, Sparrow EM. Experiments on turbulent heat transfer in a tube with circumferentially varying thermal boundary conditions. Trans ASME, J Heat Transfer 1967;89:258–68.

[2] Quarmby A, Quirk R. Measurements of the radial and tangential eddy diffusivities of heat and mass in turbulent flow in a plain tube. Int J Heat Mass Transfer 1972;15:2309–27.

[3] Maekawa H, Kawada Y, Kobayashi M, Yamaguchi H. An experimental study on the spanwise eddy diffusivity of heat in a flat-plate turbulent boundary layer. Int J Heat Mass Transfer 1991;34(8):1991–8.

[4] Kawada M, Maekawa H, Kobayashi M, Saitoh H. The effect of free-stream turbulence on spanwise eddy diffusivity of heat in a flat-plate turbulent boundary layer. JSME Int J Ser II 1992;35(4):573–9.

[5] Kobayashi M, Matsubara K, Ohki S, Maekawa H. Experimental study on a turbulent boundary layer with a constant temperature gradient for a spanwise direction. Trans Jpn Soc Mech Eng Ser B, submitted, in Japanese.

[6] Launder BE, Heat and mass transport. In: Bradshaw, editor. Topics in Applied Physics. Springer-Verlag, 1978. pp. 231–87.

[7] Rogers M, Mansour NN, Reynolds WC. An algebraic model for the turbulent flux of a passive scalar. J Fluid Mech 1989;203:77–101.

[8] Matsubara K, Kobayashi M, Maekawa H, Suzuki K. Direct numerical simulation of a turbulent channel flow with a spanwise temperature gradient (examination on the turbulence statistics). Trans Jpn Soc Mech Eng Ser B 1998;64(619):857–63, in Japanese.

[9] Kasagi N, Ohtsubo Y. Direct numerical simulation of low Prandtl number thermal field in a turbulent channel flow. In: Durst F et al., editors. Turbulent Shear Flows 8. Springer-Verlag, 1993. pp. 97–119.

[10] Kim J, Moin P. Transport of passive scalars in a turbulent channel flow. In: Andre JC et al., editors. Turbulent Shear Flows 6. Springer-Verlag, 1989, pp. 85–96.

[11] Kajishima T. Convection properties of finite difference method for convection. Trans Jpn Soc Mech Eng Ser B 1994;60(574):2058–63, in Japanese.

[12] Suzuki T, Kawamura H. Consistency of finite-difference scheme in direct numerical simulation of turbulence. Trans Jpn Soc Mech Eng Ser B 1994;60(578):3280–6, in Japanese.

[13] Kasagi N et al. Data base No. 02302043 supported by the Ministry of Education Science and Culture, 1992.

[14] Azer NZ, Chao BT. A mechanism of turbulent heat transfer in liquid metals. Int J Heat Mass Transfer 1960;1:121–38.

[15] Suzuki K. An approach to liquid metal turbulent heat transfer in a circular tube solving $\overline{v\theta}$ equation with local equilibrium assumption. Letters in Heat and Mass Transfer 1982;9(4):245–54.

[16] Suzuki K, Tohkaku A, Sato T. Liquid metal turbulent heat transfer in concentric annuli. Proc of 8th Int Heat Transf Conf 1985;3:969–74.

[17] Suzuki K, Tohkaku A. Liquid metal turbulent heat transfer in a circular tube. In: Wang BX, editor, Heat Transfer Science and Technology. Springer-Verlag, 1987. pp. 261–8.

[18] Suzuki K, Szmyd JS, Ohtsuka H. Liquid metal turbulent heat transfer in eccentric annuli. Proc 9th Int Heat Transf Conf 1990;6:299–304.

[19] Kawamura H. DNS and LES of turbulent convective heat transfer. J Heat Transf Soc Jpn 1997;36(141):4–15, in Japanese.

[20] Iida O, Kasagi N. Direct numerical simulation of homogeneous isotropic turbulence with heat transport (Prandtl number effects). Trans Jpn Soc Mech Eng Ser B 1993;59(567):3359–64, in Japanese.